Supplementary Information

Cellobiose and glucose photorefining over non-noble Bi^0-modified TiO_2 with oxygen vacancies: unraveling the effects of lignocellulosic derivatives and oxidation mechanism

Tingting Zhang[ab], Xinyao Zhang[a], Suhang Cheng[a], Dong Tian[ab], Li Zhao[ab], Jiufu Chen[c], Jinguang Hu[d] and Fei Shen[ab, *]

a. College of Environmental Sciences, Sichuan Agricultural University, Chengdu, Sichuan 611130, PR China

b. Sichuan Provincial Engineering Research Center of Agricultural Non-point Source Pollution Control, Sichuan Agricultural University, Chengdu, Sichuan 611130, PR China

c. Key Laboratory of Green Catalysis of Higher Education Institutes of Sichuan, College of Chemistry and Environmental Engineering, Sichuan University of Science and Engineering, Zigong 643000, P. R. China

d. Department of Chemical and Petroleum Engineering, University of Calgary, 2500 University Dr. NW, Calgary, AB T2N 1N4, Canada

** Corresponding author*

E-mail address: fishen@sicau.edu.cn; Tel. (Fax): +86-28-8629-3087

Experimental Section

Materials

All materials, including butyl titanate ($C_{16}H_{36}O_4Ti$), bismuth nitrate pentahydrate ($Bi(NO_3)_3 \cdot 5H_2O$), ethylene glycol ($C_2H_6O_2$), benzoquinone ($C_6H_4O_2$), glucose ($C_6H_{12}O_6$), cellobiose ($C_{12}H_{22}O_{11}$), glucaric acid ($C_6H_{10}O_8$), arabinose ($C_5H_{10}O_5$), vanillic acid ($C_8H_8O_4$), and alkali lignin, were purchased from Aladdin and were of analytical grade. They were used without further purification.

Photocatalysts Synthesis

TiO_2 precursor was synthesized through a hydrothermal method. Typically, tetrabutyl titanate was blended with absolute ethanol in a 1:4 volume ratio under vigorous stirring for 30 min to form a homogeneous precursor. Subsequently, high-purity water was added at a water-to-ethanol volume ratio of 1:20. The mixture was further stirred for 30 min before being transferred into a Teflon-lined autoclave for hydrothermal treatment at 180 °C for 12 h. The resulting product was collected, washed, and labeled as V_O-poor TiO_2.

A series of Bi^0-decorated V_O-TiO_2 catalysts with varying bismuth loadings were synthesized via a hydrothermal method. Predetermined amounts of TiO_2 precursor and bismuth nitrate pentahydrate were dispersed in 40 mL of ethylene glycol under ultrasonication. The mixture was stirred for 1 hour to form a homogeneous suspension, before transfer into a Teflon-lined autoclave and heated hydrothermally at 180 °C for 24 hours. The product was collected through filtration, thoroughly washed, and vacuum-dried. According to the mass fraction of bismuth nitrate pentahydrate (0%, 25%, 30%, 35%, and 40%), the samples were denoted as V_O-rich TiO_2 (reference TiO_2), 25-BVTO, 30-BVTO, 35-BVTO, and 40-BVTO, respectively.

Photocatalytic measurements

The photocatalytic oxidation performance of the catalysts was evaluated using glucose and cellobiose as model substrates in a phchem III photoreactor. The initial concentrations of glucose and cellobiose were set at 5 mM and 3 mM, respectively, with a catalyst loading of 20 mg. The reactions were conducted under neutral pH, in an air atmosphere with static air headspace (without active air bubbling), under magnetic stirring, using a 300 W xenon lamp as the light source with an irradiance of 87.4 mW/cm^2 (full spectrum). Prior to irradiation, the suspension was stirred in the dark for 30 minutes to establish adsorption-desorption equilibrium between the substrates and the catalyst. During the photoreaction, aliquots were collected at designated time intervals, followed by centrifugation and membrane filtration to obtain clear filtrates for subsequent analysis. Error bars were derived from replicate experimental runs. Cellobiose, glucose, and other reaction products were analyzed by high-performance liquid chromatography (HPLC, Agilent 1260 system) equipped with a refractive index detector (RID). The mobile phase consisted of a dilute sulfuric acid solution, delivered at a flow rate of 0.6 mL/min under a column temperature of 50 °C. The substrate conversion and product selectivity are calculated as follows:

$$\text{Cellobiose conversion} = \frac{[\text{cellobiose}]_0 - [\text{cellobiose}]_T}{[\text{cellobiose}]_0} \times 100\%$$

$$\text{Glucose conversion} = \frac{[\text{glucose}]_0 - [\text{glucose}]_T}{[\text{glucose}]_0} \times 100\%$$

$$\text{Glucaric acid selectivity} = \frac{[\text{glucaric acid}]_T}{[\text{cellobiose}]_0 - [\text{cellobiose}]_T} \times 100\%$$

$$\text{Arabinose selectivity} = \frac{[\text{arabinose}]_T}{[\text{glucose}]_0 - [\text{glucose}]_T} \times \frac{5}{6} \times 100\%$$

$$\text{Formic acid selectivity} = \frac{[\text{formic acid}]_T}{[\text{glucose}]_0 - [\text{glucose}]_T} \times \frac{1}{6} \times 100\%$$

$$\text{Erythrose selectivity} = \frac{[\text{erythrose}]_T}{[\text{glucose}]_0 - [\text{glucose}]_T} \times \frac{4}{6} \times 100\%$$

$$\text{Glucaric acid yield} = \frac{[\text{glucaric acid}]_T}{[\text{glucose}]_0} \times 100\%$$

$$\text{Arabinose yield} = \frac{[\text{arabinose}]_T}{[\text{glucose}]_0} \times \frac{5}{6} \times 100\%$$

$$\text{Formic acid yield} = \frac{[\text{formic acid}]_T}{[\text{glucose}]_0} \times \frac{1}{6} \times 100\%$$

$$\text{Carbon balance} = \frac{[\text{carbon in products}] + [\text{carbon inresidue substrate}]}{[\text{carbon in initial substrate}]} \times 100\%$$

Where $[\text{cellobiose or glucose}]_0$ and $[\text{cellobiose or glucose}]_T$ denote the molar concentrations of cellobiose or glucose in the initial solution and at reaction time T, respectively. $[\text{glucaric acid}]_T$, $[\text{arabinose}]_T$, $[\text{erythrose}]_T$, and $[\text{formic acid}]_T$ represent the concentrations of glucaric acid, arabinose, erythrose, and formic acid, respectively, at reaction time T. The carbon balance was calculated based on liquid products only, as gaseous carbon species could not be accurately quantified under the static headspace conditions employed.

Lignocellulosic derivatives effects investigation

Exploratory experiments were conducted to investigate the effects of lignocellulose pretreatment-derived compounds using the photo-oxidation of glucose to arabinose as a model reaction. Specifically, different concentrations of these pretreatment-derived compounds were introduced at the beginning of the photocatalytic glucose oxidation process, while all other reaction and analytical conditions were kept unchanged. All simulated pre-treatment derivatives are derived from pure chemicals.

Reactive Species Detection

Scavenging experiments were performed to identify the reactive species involved in the system. Disodium ethylenediaminetetraacetate (EDTA-2Na), isopropanol (IPA), benzoquinone (BQ), and furfuryl alcohol (FFA) were employed as specific scavengers for h^+, •OH, $•O_2^-$, and $^1O_2$, respectively, each at an initial concentration of 5 mM. The concentration of $•O_2^-$ in the photocatalytic system was semi-quantitatively analyzed using a nitroblue tetrazolium (NBT) chloride transformation assay. The initial concentration of NBT was 0.675 mM, and spectral scanning was conducted within the range of 200-500 nm.

Characterization

The microscopic morphology, elemental distribution, and surface topography of the samples were characterized using scanning electron microscopy (SEM, ZEISS Sigma 360) and atomic force microscopy (AFM, Bruker Dimension Icon). The crystal structure and surface chemical properties of the catalysts were investigated by X-ray diffraction (XRD, Rigaku Ultima IV), high-resolution transmission electron microscopy (HRTEM, JEOL JEM-F200), and X-ray photoelectron spectroscopy (XPS, Thermo Scientific K-Alpha). UV-Vis absorption spectra and photoluminescence (PL) spectra were acquired using a spectrophotometer (Shimadzu UV-3600i Plus) and a fluorescence spectrophotometer (Edinburgh FLS1000), respectively. The presence of oxygen-related radical species and defects during the photocatalytic process was detected by electron spin resonance (ESR, Bruker A300-10/12) spectroscopy. Photoelectrochemical measurements (transient photocurrent, electrochemical impedance

spectroscopy (EIS), and Mott-Schottky) were carried out on an electrochemical workstation (CHI760E) employing a standard three-electrode configuration.

Calculation

Density functional theory (DFT) calculations were carried out using the projector augmented-wave (PAW) method within the Perdew-Burke-Ernzerhof (PBE) generalized gradient approximation (GGA), as implemented in the Vienna Ab initio Simulation Package (VASP).[1-3] The work functions of the metallic Bi^0 (012) surface and the V_O-TiO_2 (101) surface were systematically evaluated. The work function (Φ) was computed according to the following equation: $\Phi = E_{vac} - E_F$, where E_F represents the Fermi energy and E_{vac} denotes the vacuum electrostatic potential.

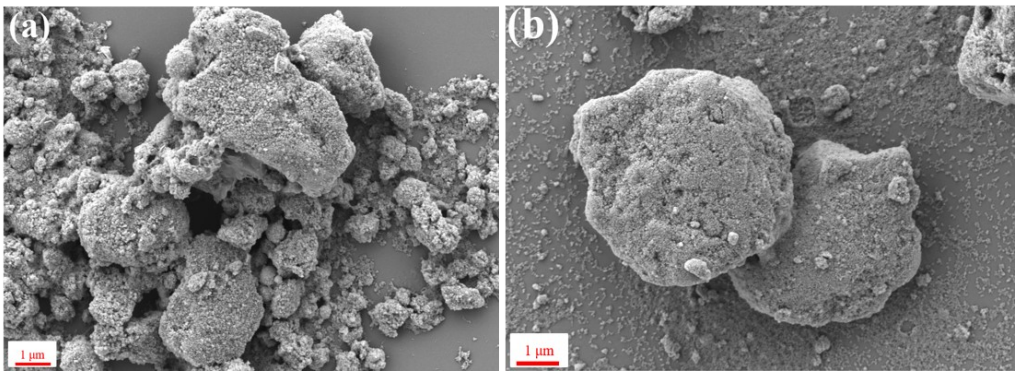

Fig. S1. SEM images of (a) V_O-poor TiO_2 and (b) V_O-rich TiO_2

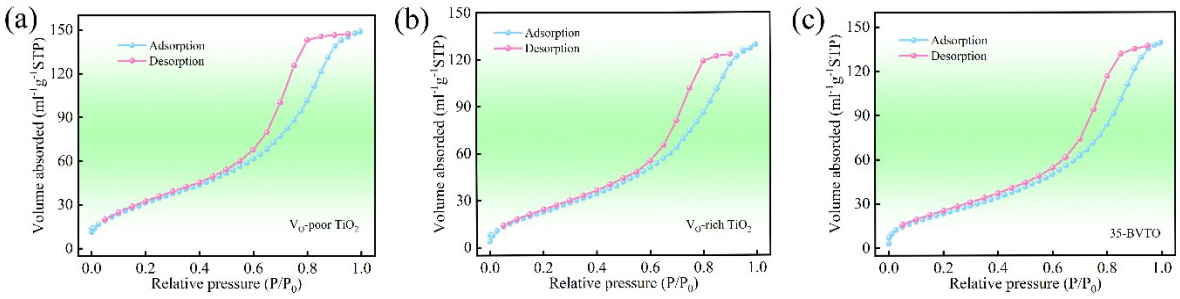

Fig. S2. Low-temperature N_2 adsorption-desorption isotherms of V_O-poor TiO_2, V_O-rich TiO_2 and 35-BVTO

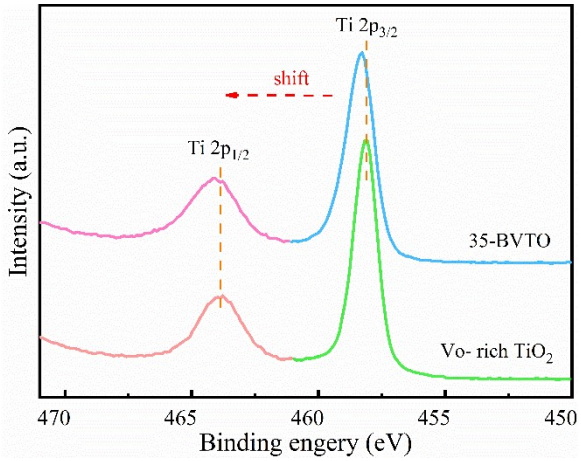

Fig. S3. High-resolution Ti 2p XPS spectra of 35-BVTO and reference TiO_2

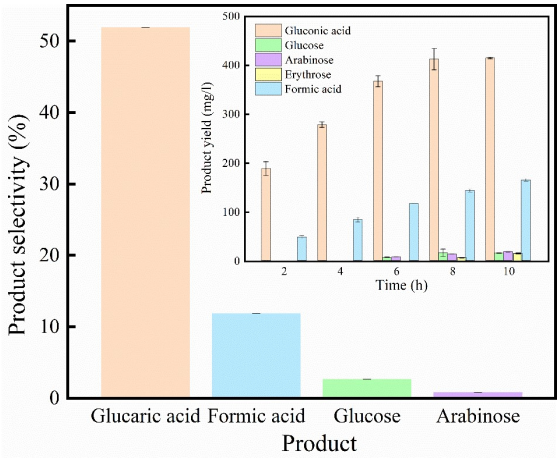

Fig. S4. Selectivity of the main product at 4 hours, inset shows yield of the main product over 10 hours.

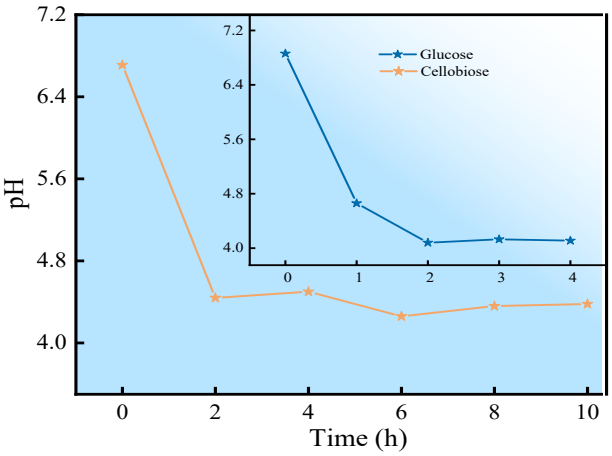

Fig. S5. Changes in pH over time in the photorefining systems of cellobiose and glucose.

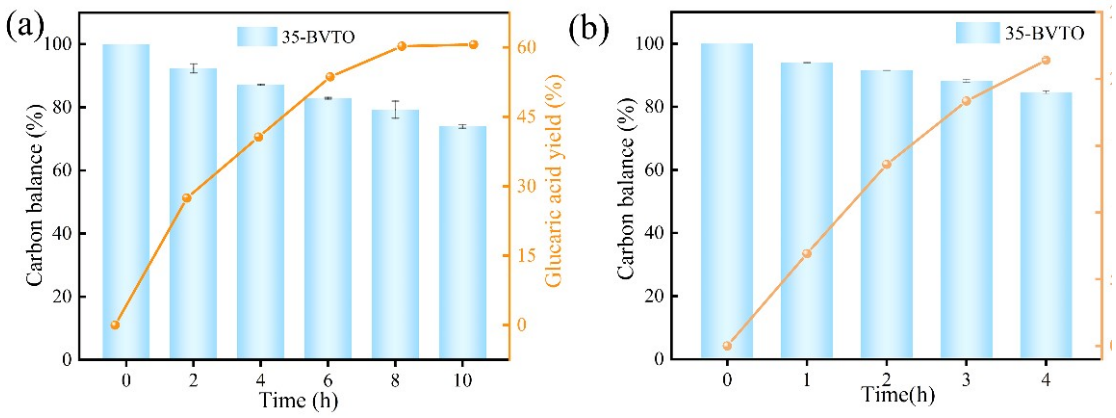

Fig. S6. Carbon balance of the photorefining process for cellobiose (a) and (b) glucose.

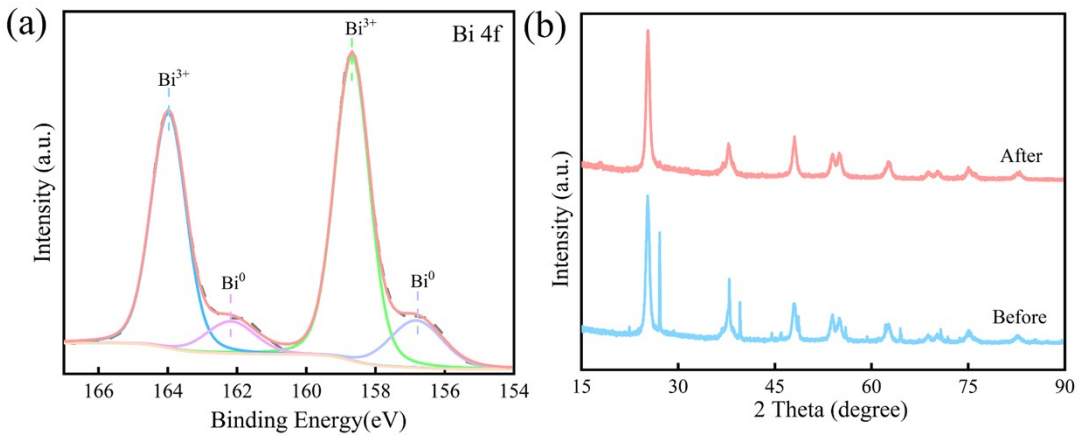

Fig. S7. High-resolution Bi 4f XPS and XRD spectra of 35-BVTO after cycling

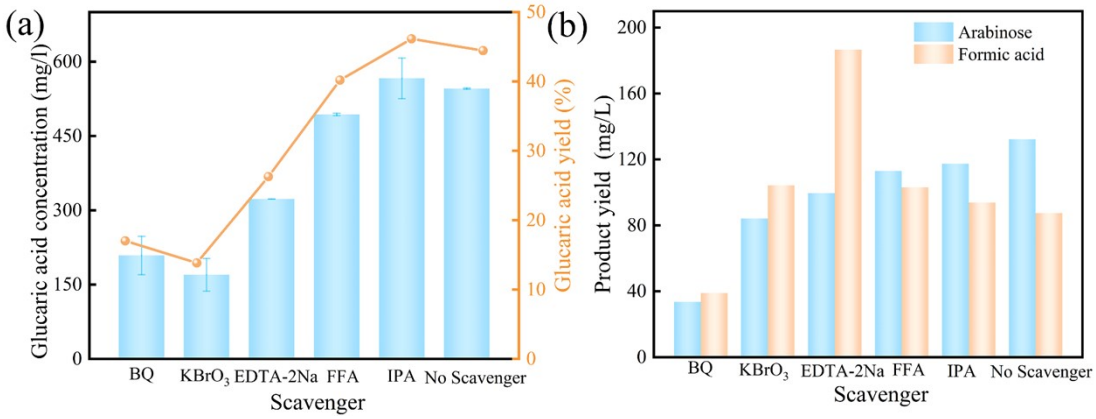

Fig. S8. (a) Changes in glucaric acid yield in the cellobiose system under different quenching agents, (b) changes in arabinose and formic acid yield in the glucose system

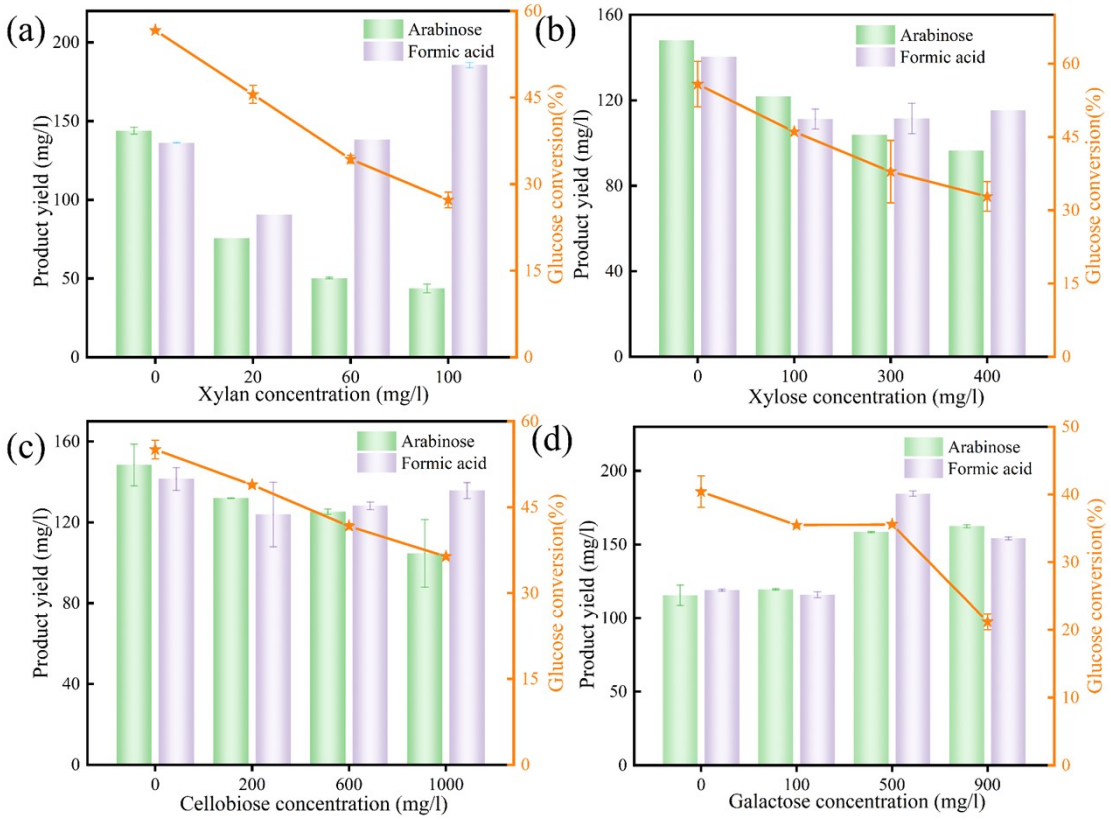

Fig. S9. Effects of various compounds on the photo-oxidative conversion of glucose to arabinose: (a) xylan, (b) xylose, (c) cellobiose, (d) galactose.

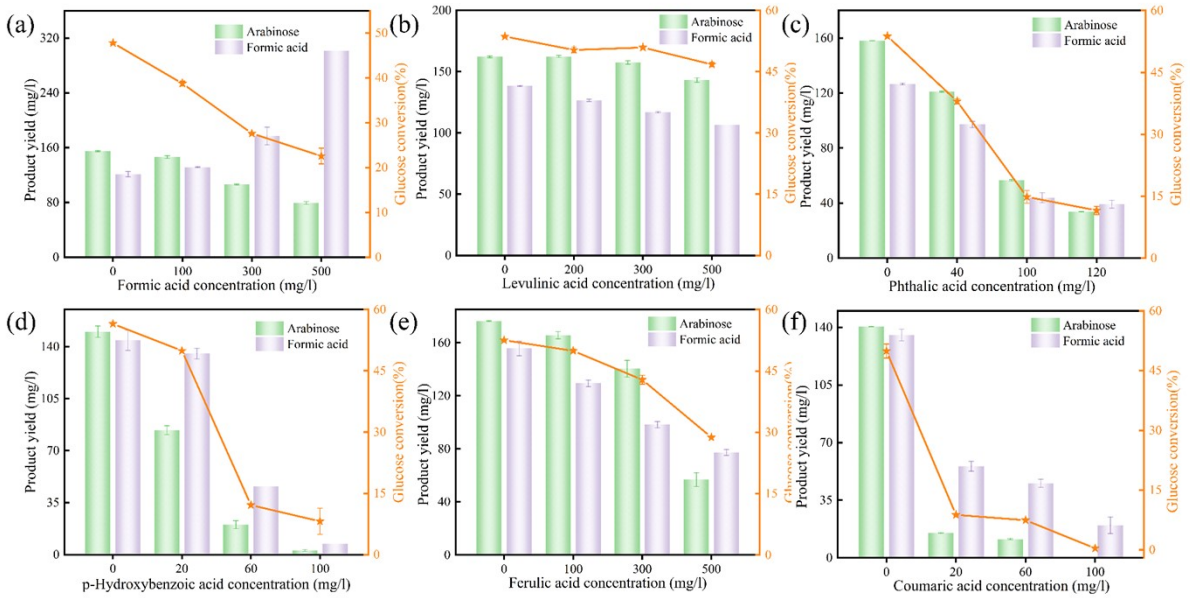

Fig. S10. Effects of various compounds on the photo-oxidative conversion of glucose to arabinose: (a) formic acid, (b) levulinic acid, (c) phthalic acid, (d) p-hydroxybenzoic acid, (e) ferulic acid, (f) coumaric acid.

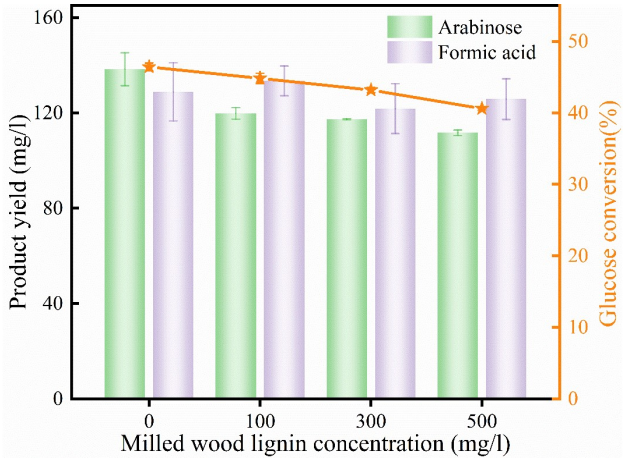

Fig. S11. Effects of milled wood on the photo-oxidative conversion of glucose to arabinose.

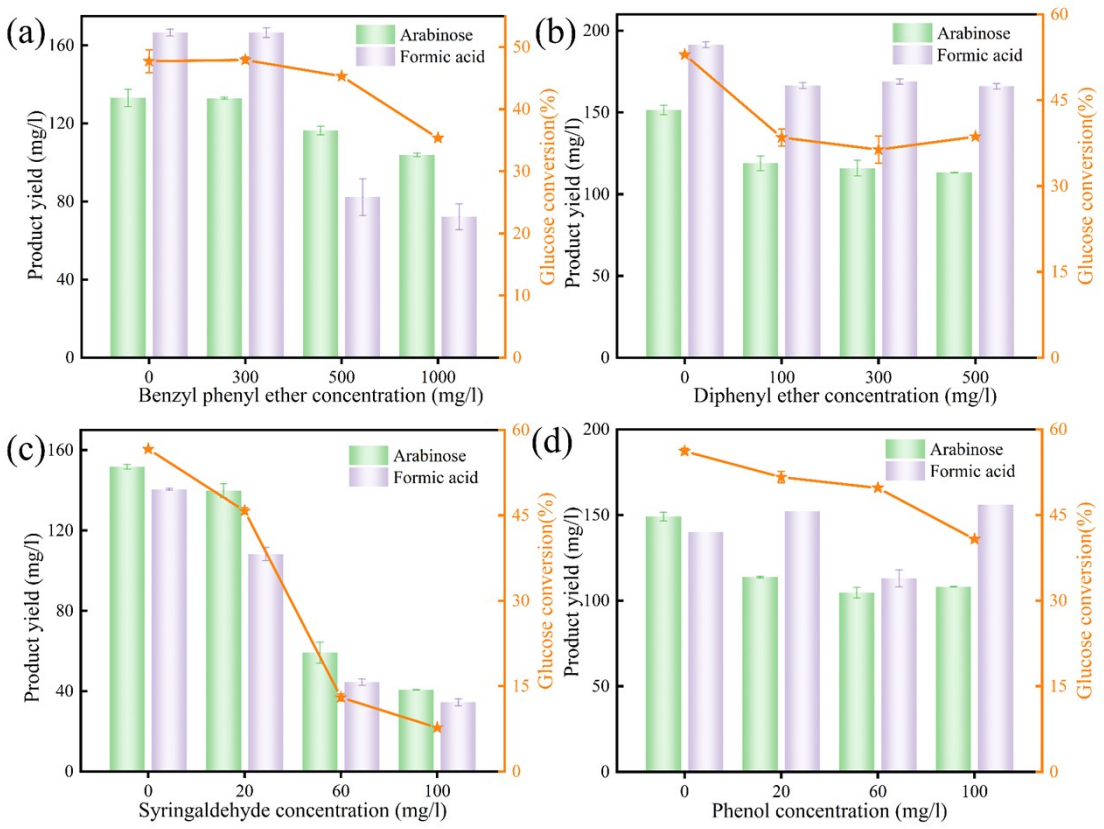

Fig. S12. Effects of various compounds on the photo-oxidative conversion of glucose to arabinose: (a) benzyl phenyl ether, (b) diphenyl ether, (c) syringaldehyde, and (d) phenol.

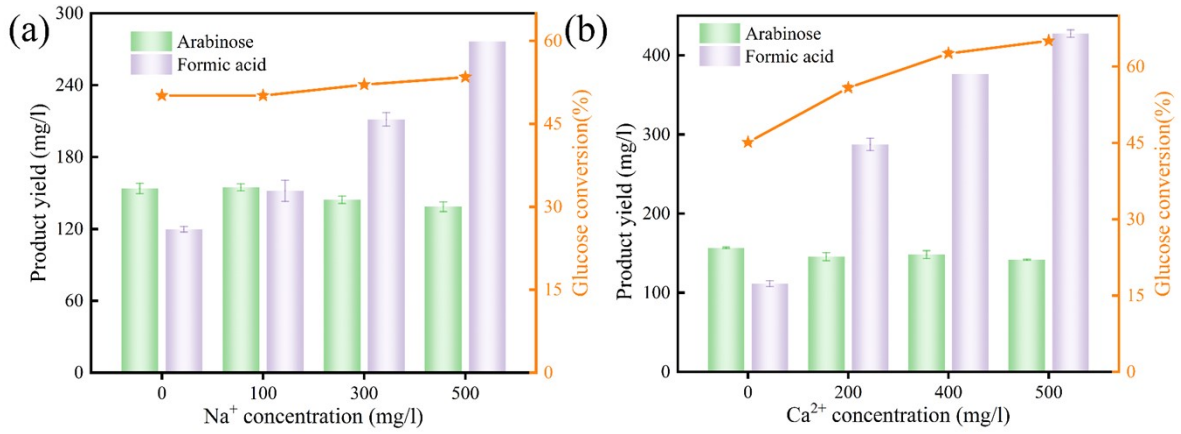

Fig. S13. Effects of various compounds on the photo-oxidative conversion of glucose to arabinose: (a) Na^{+} and (b) Ca^{2+}.

Table S1. Specific surface data for the samples

Catalysts	V_O-poor TiO_2	V_O-rich TiO_2	20-BVTO	25-BVTO	30-BVTO	35-BVTO	40-BVTO
S_{BET} (m^2/g)	124.1	95.0	71.7	75.7	89.9	93.9	108.1
V_{Pore} (cc/g)	0.233	0.204	0.170	0.174	0.191	0.216	0.222
Dv(d) (nm)	6.570	6.570	6.574	6.561	6.575	7.855	6.552

Note: Specific surface area: BET method; Pore size distribution: BJH model (adsorption branch).

Table S2. Fitting results of O 1s for V_O-rich TiO_2 and 35-BVTO

Photocatalysts	Ti-O		O-OVs		-OH	
	E_b (eV)	R_i (%)	E_b (eV)	R_i (%)	E_b (eV)	R_i (%)
V_O-rich TiO_2	529.3	80.38	530.3	14.1	531.4	5.6
35-BVTO	529.5	70.3	530.4	22.9	5314	6.8

Reference

[1] J. Hafner, J. Comput. Chem., 2008, **29**, 2044-2078.

[2] C. Qin, X. Tang, J. Chen, H. Liao, J. Zhong, J. Li, Colloid. Surface. A., 2021, **617**, 126224.

[3] T. Zhang, Y. Chen, X. Yang, J. Chen, J. Zhong, J. Li, M. Li, Mater. Today. Chem., 2023, **28**, 101358.